

[Article ID] 1003- 6326(2002) 04- 0720- 03

Crystallization behavior of melt-spun NdFeB permanent magnets^①

XU Hui(徐 晖), NI Jian-sen(倪建森), ZHU Ming-yuan(朱明原),
ZHOU Bang-xin(周邦新), DONG Yuan-da(董远达), XIAO Xu-shan(肖学山)

(Institute of Materials Science and Engineering, Shanghai University, Shanghai 200072, China)

[Abstract] The crystallization behavior of melt-spun $\text{Nd}_{8.5}\text{Fe}_{78}\text{Co}_5\text{Cu}_1\text{Nb}_1\text{B}_{6.5}$ ribbons was investigated using dynamic differential scanning calorimetry (DSC) and X-ray diffractometry (XRD). It was found that the as-spun ribbons crystallize in two steps: at first the $\text{Nd}_3\text{Fe}_{62}\text{B}_{14} + \alpha\text{-Fe}$ phases are formed and subsequently $\text{Nd}_3\text{Fe}_{62}\text{B}_{14}$ transformed to $\text{Nd}_2\text{Fe}_{14}\text{B}$ and $\alpha\text{-Fe}$ upon heating above 680 °C. The effective activation energy of two crystallization peaks are 332.0 kJ/mol and 470.5 kJ/mol, respectively. As the wheel speed increases, the magnetic properties of the magnet change obviously. When the wheel speed is 18 m/s, the best magnetic properties of the magnet was obtained after the sample was annealed at 690 °C for 8 min: $B_r = 0.74\text{T}$, $iH_c = 421.7\text{ kA/m}$, $(BH)_{\max} = 64.5\text{ kJ/m}^3$.

[Key words] nanocomposite magnet; crystallization behavior; activation energy

[CLC number] TG 132.2; TM 273

[Document code] A

1 INTRODUCTION

Since the discovery of remanence enhancement in isotropic nanocrystalline $\text{Nd}_{4.5}\text{Fe}_{77}\text{B}_{18.5}$ alloy in 1988 by Coehoorn et al^[1, 2], nanocomposite NdFeB magnet have received great attention in the past years^[3~6]. Besides it possesses good hard magnetic properties, the reduction in the rare earth amount also reduces its costs, thereby causing increased interest for practical applications.

Magnetic characteristics of the nanocomposite magnets are influenced sensitively by their microstructures such as the volume ratio of hard to soft magnetic phases, the grain sizes and their uniform distribution^[7, 8]. Since the order of formation and growth rate of each phase, $\text{Nd}_2\text{Fe}_{14}\text{B}$, Fe_3B and $\alpha\text{-Fe}$ are different, it is the key technology to get the optimum microstructure in the nanocomposite materials. Therefore, in this study, the thermal behavior and magnetic properties of $\text{Nd}_{8.5}\text{Fe}_{78}\text{Co}_5\text{Cu}_1\text{Nb}_1\text{B}_{6.5}$ alloy are studied.

2 EXPERIMENTAL

The alloy composition in this investigation was $\text{Nd}_{8.5}\text{Fe}_{78}\text{Co}_5\text{Cu}_1\text{Nb}_1\text{B}_{6.5}$ (mole fraction, %). The alloy was initially melted in vacuum induction furnace and subsequently casted into bar, which was subsequently annealed at 1 000 °C for 8 h. For melt-spinning, the alloy bar was crushed into pieces less than 8 mm in height.

The pieces were melt-spun in ZK-10TCIII vacuum flash hardening furnace with wheel speeds (v_s) ranging from 9.8 to 36.7 m/s. The phase identification was carried out by X-ray diffractometry and the

mean grain size was determined by using the Scherrer formula. The crystallization behaviors of as-quenched ribbon were detected by Perkin-Elmer DSC7. The melt spun ribbons were annealed at 570~ 810 °C for 8 min. The ribbons were grind and the powder of which was bonded with 4% (mass fraction) epoxy resin and compressed to shape of $d 10\text{ mm} \times 10\text{ mm}$. The density of bonded compact magnet was about 6.1 g/cm^3 . The magnetic properties of bonded magnets were measured in a DGY-2C magnetometer at room temperature.

3 RESULTS AND DISCUSSION

X-ray diffraction spectra for the $\text{Nd}_{8.5}\text{Fe}_{78}\text{Co}_5\text{Cu}_1\text{Nb}_1\text{B}_{6.5}$ alloy as a function of wheel speeds (v_s) are shown in Fig. 1. It shows that when the wheel speed is 9.8 m/s, $\alpha\text{-Fe}$, $\text{Nd}_2\text{Fe}_{14}\text{B}$,

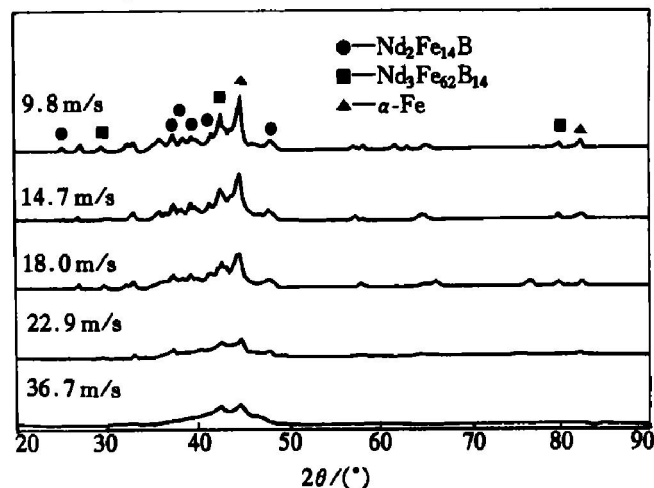


Fig. 1 X-ray diffraction spectra for $\text{Nd}_{8.5}\text{Fe}_{78}\text{Co}_5\text{Cu}_1\text{Nb}_1\text{B}_{6.5}$ alloy melt-spun at different wheel speeds

① **[Foundation item]** Special Item for Nanomaterials (0152nm020) supported by the Shanghai Municipal Developing Foundation of Science & Technology **[Received date]** 2001- 10- 08

$\text{Nd}_3\text{Fe}_{62}\text{B}_{14}$ phases and some amorphous phase are obtained. With increasing wheel speed v_s , the intensities of diffraction peaks from crystalline phases decrease and the content of the amorphous phase increases. When the wheel speed is 36.7 m/s, the diffraction lines of crystalline phases disappear, and only a wide diffuse amorphous peak is observed.

Fig. 2 shows the DSC curves of the amorphous $\text{Nd}_{8.5}\text{Fe}_{78}\text{Co}_5\text{Cu}_1\text{Nb}_1\text{B}_{6.5}$ alloy with wheel speed of 36.7 m/s. Two gentle exothermic peaks are observed in the curves, indicating that the crystallization of the $\text{Nd}_{8.5}\text{Fe}_{78}\text{Co}_5\text{Cu}_1\text{Nb}_1\text{B}_{6.5}$ amorphous alloys took place through two stages. θ_{p1} and θ_{p2} of Fig. 2 indicate the exothermic peak temperatures of the two exothermic reactions, respectively.

To identify the first and the second transformations, the $\text{Nd}_{8.5}\text{Fe}_{78}\text{Co}_5\text{Cu}_1\text{Nb}_1\text{B}_{6.5}$ amorphous samples are annealed for 8 min at 580 °C and 680 °C, respectively, and then the phase is examined by XRD (as shown in Fig. 3). The samples annealed at 580 °C showed the presence of αFe and $\text{Nd}_3\text{Fe}_{62}\text{B}_{14}$ phases, and some amorphous phase still remain in the sample. However, when the sample is annealed at 680 °C, the sample is completely crystallized, αFe and $\text{Nd}_2\text{Fe}_{14}\text{B}$ phases were observed. The diffraction peaks of $\text{Nd}_3\text{Fe}_{62}\text{B}_{14}$ phase disappear, and the intensity of diffraction peaks for αFe phase increases. Therefore, the first exothermal peak in Fig. 2 is the transformation from amorphous materials to αFe and $\text{Nd}_3\text{Fe}_{62}\text{B}_{14}$ phase, and the second exothermal peak in Fig. 2 is the $\text{Nd}_3\text{Fe}_{62}\text{B}_{14}$ phase transformation to αFe and $\text{Nd}_2\text{Fe}_{14}\text{B}$.

According to the DSC data, the effective activation energy of two crystallization peaks in Fig. 2 are calculated to be 332.0 kJ/mol and 470.5 kJ/mol, respectively.

Fig. 4 shows the relationship between magnetic

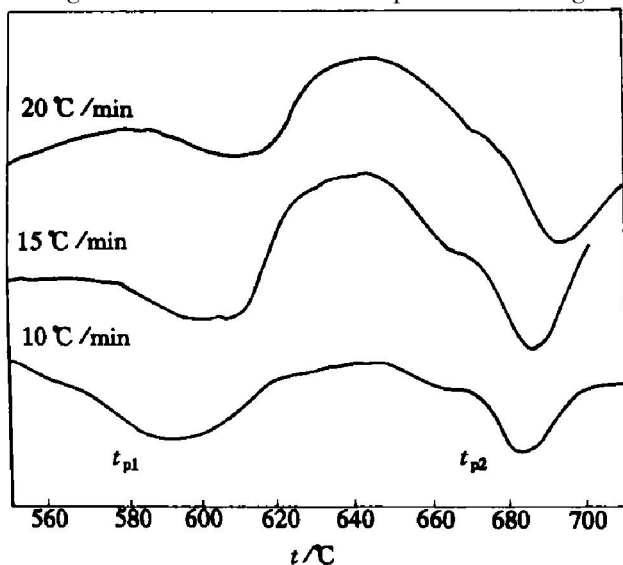


Fig. 2 DSC curves of amorphous $\text{Nd}_{8.5}\text{Fe}_{78}\text{Co}_5\text{Cu}_1\text{Nb}_1\text{B}_{6.5}$ alloy with wheel speed of 36.7 m/s

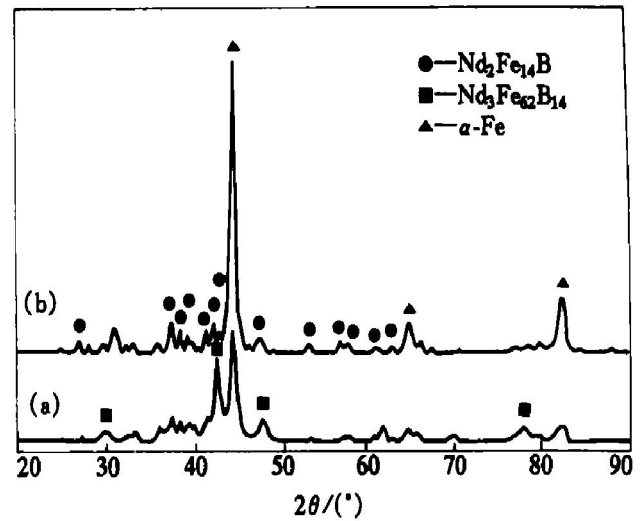


Fig. 3 X-ray diffraction spectra of $\text{Nd}_{8.5}\text{Fe}_{78}\text{Co}_5\text{Cu}_1\text{Nb}_1\text{B}_{6.5}$ amorphous alloy annealed at different temperatures for 8 min (a) -580 °C; (b) -680 °C

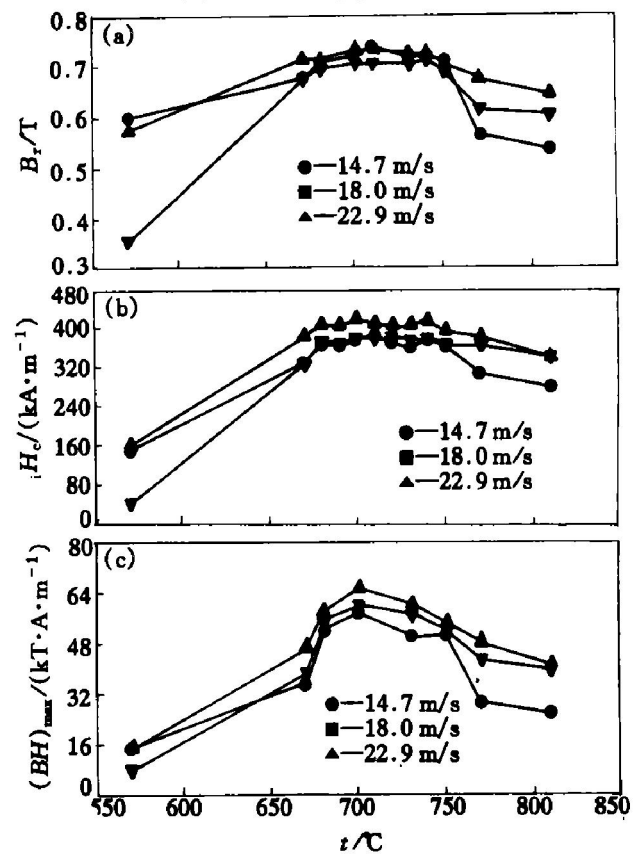


Fig. 4 Magnetic properties of $\text{Nd}_{8.5}\text{Fe}_{78}\text{Co}_5\text{Cu}_1\text{Nb}_1\text{B}_{6.5}$ alloy annealed at different temperatures for 8 min with different wheel speeds

properties of $\text{Nd}_{8.5}\text{Fe}_{78}\text{Co}_5\text{Cu}_1\text{Nb}_1\text{B}_{6.5}$ bonded magnet and the annealing temperatures for different wheel speeds (14.7~22.9 m/s).

It is obvious that magnetic properties of bonded magnet were affected by changing the wheel speed and heat treated temperature. The magnetic properties of bonded magnet increase with increasing annealing temperature from 570 °C at the beginning then decrease gradually at 730 °C. Excellent magnetic

properties of bonded magnet were obtained with wheel speed of 18 m/s annealed at 690 °C for 8 min, $B_r = 0.74\text{T}$, $H_c = 421.7\text{ kA/m}$, $(BH)_{\max} = 64.5\text{ kJ/m}^3$. At that time, the mean grain size of the two-phase was about 50 nm.

4 CONCLUSIONS

1) The crystallization process of melt-spun $\text{Nd}_{8.5}\text{Fe}_{78}\text{Co}_5\text{Cu}_1\text{Nb}_1\text{B}_{6.5}$ alloy takes place through two steps, at first the $\text{Nd}_3\text{Fe}_{62}\text{B}_{14}$ -type + $\alpha\text{-Fe}$ phases are formed and subsequently $\text{Nd}_3\text{Fe}_{62}\text{B}_{14}$ phase transformed to $\text{Nd}_2\text{Fe}_{14}\text{B}$ and $\alpha\text{-Fe}$ upon heating above 680 °C. The effective activation energy of two crystallization peaks are 332.0 kJ/mol and 470.5 kJ/mol, respectively.

2) When the wheel speed is 18m/s, the excellent magnetic properties of the magnet was obtained after the sample was annealed at 690 °C for 8 min. $B_r = 0.74\text{T}$, $H_c = 421.7\text{ kA/m}$, $(BH)_{\max} = 64.5\text{ kJ/m}^3$.

[REFERENCES]

[1] Coehoom R, de Mooij D B, Duchtean J P W B, et al.

Novel permanent magnetic materials made by rapid quenching [J]. *J de Phys*, 1988, 49: 669– 670.

- [2] Coehoom R, de Mooij D B, Waard C D E. Meltspun permanent magnet materials containing Fe_3B as the main phase [J]. *J Magn Mater*, 1989, 80: 101– 104.
- [3] Skomski R, Coey J M. Nucleation field and energy product of aligned two-phase magnets—progress towards the 1MJ/m^3 magnet [J]. *IEEE Trans Magn*, 1993, 29: 2860– 2862.
- [4] Schrefl T, Fidler J, Kronmuller H. Remanence and coercivity in isotropic nanocrystalline permanent magnets [J]. *Phys Rev B*, 1994, 49: 6100– 6110.
- [5] Chang W C, Wu S H, Ma B M, et al. Magnetic properties enhancement of $\alpha\text{-Fe}/\text{Nd}_2\text{Fe}_{14}\text{B}$ -type nanocomposites by Co substitution [J]. *J Appl Phys*, 1998, 83: 2147– 2450.
- [6] Gao Y H, Zhu J H, Yang C J, et al. Thermomagnetic behaviors of $\text{Nd}_2\text{Fe}_{14}\text{B}/\text{Fe}_3\text{B}$ based nanocomposite magnets [J]. *J Magn Magn Mater*, 1998, 186: 97– 103.
- [7] Yang C J, Park E B. The effect of magnetic field treatment on the enhanced exchange coupling of a $\text{Nd}_2\text{Fe}_{14}\text{B}/\text{Fe}_3\text{B}$ magnet [J]. *IEEE Trans Magn*, 1996, 32: 4428 – 4430.
- [8] Yang C J, Park E B. The effect of magnetic field treatment on the enhanced exchange coupling of a $\text{Nd}_2\text{Fe}_{14}\text{B}/\text{Fe}_3\text{B}$ [J]. *J Magn Magn Mater*, 1997, 166: 243– 248.

(Edited by YANG Bing)